The Molecular Structure and Hydrogen Bond Geometry in Liquid Formamide: Electron, Neutron, and X-Ray Diffraction Studies

E. Kálmán, I. Serke, and G. Pálinkás

Central Research Institute for Chemistry of the Hungarian Academy of Sciences, Budapest

M. D. Zeidler and F. J. Wiesmann

Institut für Physikalische Chemie der Rheinisch-Westfälischen Technischen Hochschule, Aachen

H. Bertagnolli

Institut für Physikalische Chemie der Universität, Würzburg

P. Chieux

Institut Max von Laue–Paul Langevin, Grenoble

Z. Naturforsch. **38a**, 231–236 (1983); received October 4, 1982

Dedicated to Professor Alfred Klemm on the occasion of his 70th birthday

Electron, neutron and X-ray diffraction patterns of liquid formamide have been measured at a temperature of 25 °C. Analysis of the diffraction data yields the molecular structure and the average geometry of the hydrogen bond. The molecular parameters obtained from liquid diffraction experiments are in good agreement with those from gas electron diffraction for the free molecule. The mean O...N and O...H hydrogen bond distances are 2.9 Å and 1.9 Å, respectively. Four H-bonds per molecule are found on the average. The deviation of the H-bonds from the linearity is estimated.

I. Introduction

The molecular structure of formamide was determined in the vapour phase by Kitano and Kuchitsu using electron diffraction [1] and in the molecular crystal by Ladell and Post [2] using X-ray diffraction. A comparison between the bond distances of the planar molecule in both phases shows a lengthening of about 0.07 Å of C–N and a shortening of about 0.04 Å of C=O bonds in the gas phase. The increase and decrease in double bond character of the C–N and C=O bonds can be ascribed to the strong hydrogen bonds in the crystal.

The crystal structure of formamide consists of puckered sheets of formamide molecules [2]. Within the sheets, pairs of formamide molecules associate around the symmetry centers to form almost coplanar dimers. Within each sheet two types of hydrogen bond are found. One of them is 2.93 Å long and links molecules together to form bimolecular units, the other one, which is 0.05 Å shorter (i.e. 2.88 Å), links the bimolecular units together to form sheets. It is reasonable to suppose that the longer bond in the crystal is also weaker and can more easily be broken on melting.

Indications concerning the structure of liquid formamide were obtained from ^{1}H NMR chemical shift measurements [3]. These measurements indicate a tetramer structure with a cyclic dimer(1-cis tetramer). Other indications for the structure of the liquid were obtained by comparing theoretical results with ESCA data [4]. This comparison allowed both linear chains and a 1-cis tetramer. Ab initio calculations [5] led to the conclusion that the dominant unit in the structure of liquid formamide should contain both a cyclic dimer and linear chains. The same was concluded from the infrared and Raman studies [6]. Two X-ray studies on liquid formamide are known already. The first one has been done by De Sando and Brown [7]. The authors assigned to the N...O interaction a length of 3.05 Å and suggested that formamide in the liquid state has a short range order which resembles that in the crystalline state. A second X-ray study has been reported by Ohtaki [8] in this year. He concludes that the formamide molecules form in the liquid an open-chain structure. The ring structure found in the solid phase has not been observed.

Reprint requests to Dr. E. Kálmán, 1525 Budapest, P.O. Box 17, Hungary.

0340-4811 / 83 / 0200-0231 $ 01.3 0/0. – Please order a reprint rather than making your own copy.

As a part of a systematic study of liquid amides, we present here results of combined electron, neutron and X-ray scattering experiments, concerning the structure of molecules and the geometry of hydrogen bonds in liquid formamide. The hydrogen bond geometry will be discussed in the present paper while a detailed analysis of the liquid structure following from this geometry will be given in another paper.

II. Experimental and Data Evaluation

The differential cross section for 68 keV electrons ($\lambda = 0.05$ Å) scattering by liquid formamide was measured at 25 °C using a special electron diffraction apparatus for liquid samples described in detail earlier [9]. Briefly, the main part of the equipment is a chamber under pressure producing a stable thin liquid film for the diffraction of a penetrating electron beam. The scattering of liquid formamide was measured with three different camera lengths and their normalization in overlapping ranges of the scattering variable resulted in a scattering intensity function ranging from 0.7 $Å^{-1} \leqq k \leqq 23.6$ $Å^{-1}$ (scattering variable $k = (4\pi/\lambda)\sin\vartheta$). In order to compensate the predominance of scattering at small angles a rotating sector was used [10]. Diffraction patterns were recorded on photoplates. During the experiments the temperature and pressure in the chamber were controlled. Optical absorbancies were measured by a microdensitometer. The absorbancies were converted into intensities using the intensity-density characteristics of Agfa-Gevaert photoplates. The measured intensities were corrected for extraneous scattering (blank plate) of the apparatus, for the sector shape and flat plates [11]. The intensity functions were determined at equal spacings in k by Lagrangian interpolation. The separation of the structure independent background scattering, which is composed of atomic self-scattering, inelastic scattering and multiple scattering and also the conversion of the experimental intensities to absolute scale were carried out by an iterative procedure together with a refinement of the parameters of the molecular structure.

Neutron scattering studies of the deuterized liquid formamide $CDOND_2$ were carried out at 25 °C and with a wavelength of 0.7 Å. The scattering intensities were measured with the diffractometer D4 at the high-flux reactor of the Institute Laue-Langevin, Grenoble. The liquid was placed in vacuum-tight vanadium cylinders. The angular range $1.2° \leqq 2\vartheta \leqq 110°$ was covered at intervals of 0.1875 using a multidetector and the average counting level achieved was 2000 counts per point. Additional runs with the empty container and a background run were also performed. The experimental data were corrected for background, container, selfabsorption, multiple scattering and inelasticity. The data were converted to an absolute scale by determining a normalization factor from a vanadium run. The details of the correction procedure are described elsewhere [12–14].

X-ray diffraction measurements were carried out on flat plane-parallel specimens using transmission geometry and MoK_α ($\lambda = 0.711$ Å) radiation monochromated by a flat LiF crystal in the primary beam. The plane parallel windows of the specimen holder thermostated at 25 °C have been prepared from 0.1 mm thick plates of a quartz single crystal. The scattering data were measured in the range of the scattering variable 0.3 $Å^{-1} \leqq k \leqq 14.5$ $Å^{-1}$. The measured intensities were corrected for background, polarization, absorption and Compton scattering. The intensity of the scattered X-rays was collected at equidistant steps with an increment $\Delta k = 0.05$ $Å^{-1}$ and $2 \cdot 10^5$ impulses at each point. The absolute scale was established by the method of Krogh-Moe and by the high angle method.

The details of the data processing and correction procedure are discussed in [15].

The normalized intensities for experimentally not accessible values were extrapolated empirically to $k = 0$ using the limiting value $I(0)$ calculated from the isothermal compressibility of 3.736×10^{-10} $m^2 N^{-1}$.

The total experimental structure functions were determined for all three types of experiment by the following relation:

$$H^{\alpha}(k) = \frac{I^{\alpha}_{\text{norm}}(k) - I^{\alpha}_{\text{self}}(k)}{\left|\sum_i f_i^{\alpha}\right|^2}, \qquad (1)$$

where $I^{\alpha}_{\text{norm}}(k)$, $I^{\alpha}_{\text{self}}(k)$, $f_i^{\alpha}(k)$ are respectively the normalized coherent intensities, calculated self scattering of the atoms in one formamide molecule and tabulated [14–17] coherent scattering amplitudes for atoms i. Index α stands for the three different types of diffraction experiments. A final correction to eliminate systematic errors, arising from inaccuracies in correction, was applied to the experimental structure functions [11–12].

III. The Molecular Structure

The total structure functions derived from experiments may be written as the sum of two terms:

$$H(k) = H_m(k) + H_d(k) . \quad (2)$$

The first term in Eq. (2) is the molecular part of the scattering due to independent molecules. The second term is the distinct part of the scattering which contains contributions from intermolecular spatial and orientational correlations. Since the distinct structure function $H_d(k)$ decays much faster to zero than the molecular structure function H_m, the large k behaviour of the total structure function $H(k)$ in the upper k-range is determined by its molecular component i.e. $H(k) \cong H_m(k)$. This property of the total structure functions can be used for determination of the molecular structure by a least-square fitting of the following analytical expression for the molecular structure function to the large k part of the total structure function [11, 18].

$$H_m(k) = \sum_{i \neq j} \frac{f_i(k)\, f_j(k)}{\left|\sum_i f_i\right|^2} j_0(k r_{ij}) \exp\{-l_{ij}^2 k^2/2\}, \quad (3)$$

where r_{ij}, l_{ij} are the intramolecular distances and the root mean square amplitudes of distances, j_0 is the spherical Bessel function of zero order.

Since the measured electron structure function $H^{ED}(k)$ is given in a wide range of the scattering variable k, we have used this method to determine the structure of formamide molecules by least-squares refinement of expression (3) against the

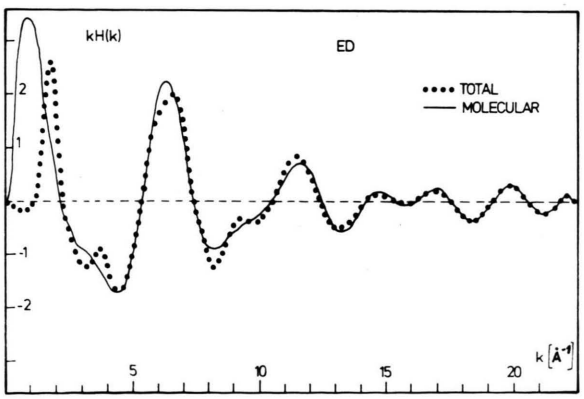

Fig. 1. The k weighted experimental and molecular structure functions from electron diffraction. The molecular structure function is fitted to the experimental one in the range 7 Å$^{-1} \leqq k \leqq$ 22.5 Å^{-1}.

7 Å$^{-1} \leqq k \leqq$ 22.5 Å^{-1} range of the $H^{ED}(k)$. The function $kH_m(k)$ for liquid formamide together with the total electron structure function is shown in Figure 1. The two curves are in agreement for values $k \geqq 8$ Å^{-1}, except for small deviations at lower values of k, which are due to the contributions of the H-bond interactions. In order to have an independent determination of the molecular parameters, the X-ray molecular structure function was derived by another method based on the properties of the total pair correlation function, $G(r)$, given by the following relation:

$$G(r) = 1 + (2\pi^2 \varrho_0)^{-1} \int_0^\infty k^2 H(k)\, j_0(kr)\, dk, \quad (4)$$

where ϱ_0 is the number density.

Regarding Eq. (2), $G(r)$ can also be written as the sum of molecular and distinct terms

$$G(r) = G_m(r) + G_d(r). \quad (5)$$

If there is no overlap between the intramolecular and intermolecular distance contributions, Eq. (5) renders possible the separation of the $G_m(r)$ function.

The total X-ray pair correlation function (not shown in this paper) approached a value of zero at a distance of 2.6 Å. Because no intermolecular contributions, except O...H interactions were expected in the total X-ray pair correlation function below $r = 2.6$ Å, an "experimental" molecular structure function $H_m^* k$ was derived by inverse Fourier transformation of $G(r)$ in the range $0 \leqq r \leqq 2.6$ Å. The parameters $r_{\alpha\beta}$ and $l_{\alpha\beta}$ for the molecular structure were then obtained by least-squares refinement of expression (3) against the $H_m^*(k)$ function in the range $0 \leqq k \leqq 13.5$ Å^{-1}. The molecular structure function $H_m(k)$, calculated from these parameters, is shown in Fig. 2, together with the $H_m^*(k)$ molecular structure function calculated from the molecular part of $G(r)$ and the total X-ray structure function derived from experiment. The molecular parameters obtained from both electron and X-ray scattering data are listed in Table 1. For comparison, the results obtained by gas electron diffraction for the free molecule [1] are also presented in Table 1.

The molecular parameters resulting from the liquid electron diffraction experiment are in good agreement with those from liquid X-ray and gas electron diffraction. The structure of the formamide

Table 1. Mean distances r, rms variations l in Å and bond angles for the formamide molecule in vapour [1] and liquid phase.

	Ref. [1]		ED		XD	
	r	l	r	l	r	l
C=O	1.212(3)	0.039	1.213(6)	0.067	1.219(6)	0.065
C–N	1.368(3)	0.043	1.360(10)	0.067	1.375(10)	0.062
C–H	1.125(12)	0.080	1.120(22)	0.076	1.125[a]	0.080[a]
N–H	1.027(6)	0.090	1.020(15)	0.077	1.027[a]	0.090[a]
< OCN	125.0(4)		125.2(5)		124.2(5)	
< NCH	112.7(1)		112.7[a]		112.7[a]	
< CNHC	118.7(1)		118.7[a]		118.7[a]	
< CNHT	119.7(1)		119.7[a]		119.7[a]	

[a] Values were kept constant in the fitting procedure.

molecule is found to be the same as that of a free molecule. Changes of the double bond characters of the C–N and C=O bonds appearing in the crystal [2] are not observable in the liquid phase.

The molecular structure function for neutron scattering has been calculated from the parameters listed in Table 1 for electron diffraction.

IV. The Hydrogen Bond Interactions

The distinct structure functions $H_d^x(k)$ are now obtained as the difference between the total structure functions and the molecular terms $H_d^x(k) = H^x(k) - H_m^x(k)$. The three $H_d^x(k)$ functions (ND, ED, XD) are presented in Figure 3.

The most striking feature of these functions is the presence of oscillations in the large k range. This feature is characteristic for H-bonded molecular liquids [18].

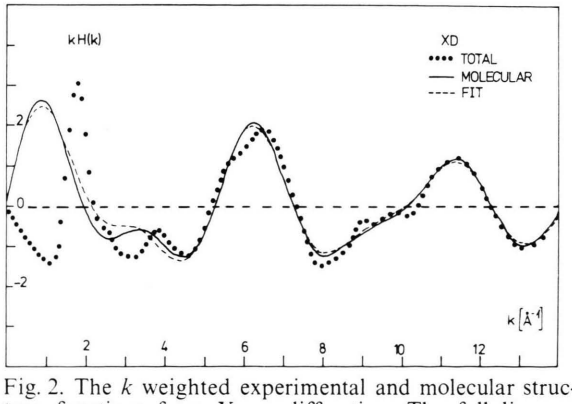

Fig. 2. The k weighted experimental and molecular structure functions from X-ray diffraction. The full line represents the numerical Fourier transform of the intramolecular peaks in the total pair correlation function. The dashed line shows the fitted molecular structure function.

Simple molecular liquids as CCl_4 and CS_2 [19, 20] yield distinct structure functions which decay to zero much faster, almost no oscillations could be detected for $k > 6$ Å^{-1}. Based on this argument we assume that at high k values the O...N and O...H H-bond interactions contribute most to the $H_d(k)$ functions

$$H_d(k) \approx H_{\text{H-bond}}(k) = H_{\text{O...N}}(k) + H_{\text{O...H}}(k).$$

By least-squares fitting of expression (3) to the large k part of the distinct structure functions beyond $k \geqq 4$ Å^{-1}, we have obtained the structural parameters of H-bond interactions listed in Table 2. The H-bond structure functions calculated from the parameters given in Table 2 for the three different scattering experiments are also shown in Figure 3. As a result of the calculations beyond $k = 6$ Å^{-1} good agreement can be observed between the distinct structure functions and their H-bond contributions. The distinct pair correlation functions derived by Fourier transformations from the $H_d(k)$ functions are shown in Figure 4 together with $G_{\text{H-bond}}(r)$ contributions.

Table 2. Mean O...N and O...H intermolecular distances (r) and associated rms variations (l) in Å and average number of H-bonds per molecule (n).

		r	l	n
ED	O...N	2.90(1)	0.161	4.08
	O...H	1.90(1)	0.147	4.00
ND	O...N	2.90(4)	1.169	4[a]
	O...H	1.90(2)	0.152	3.9
XD	O...N	2.92(4)	0.175	3.54
	O...H	1.93(6)	0.070	4[a]

[a] Values were kept constant.

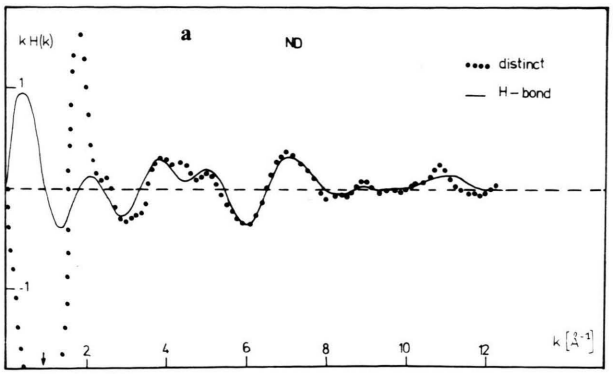

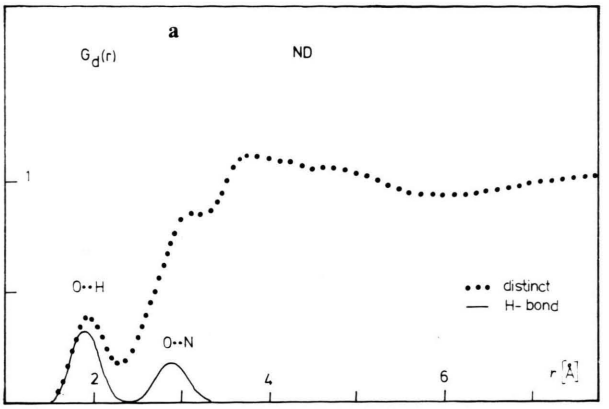

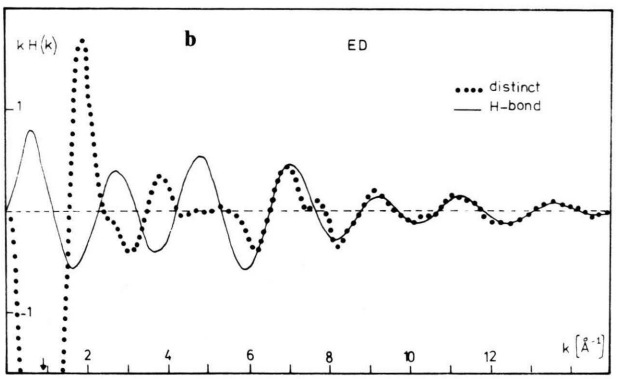

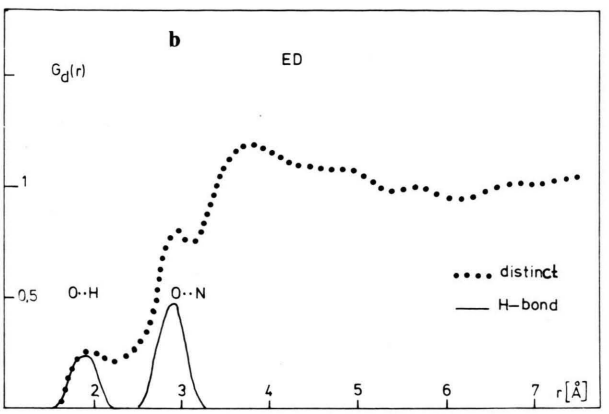

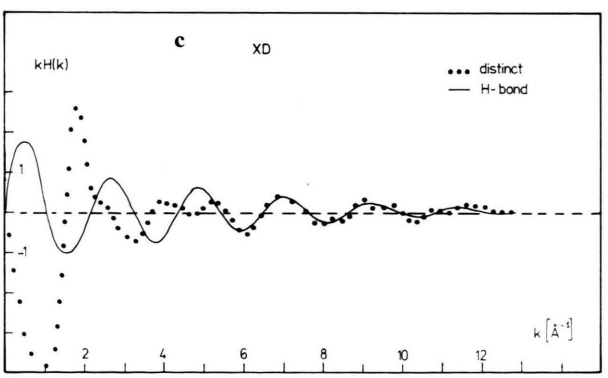

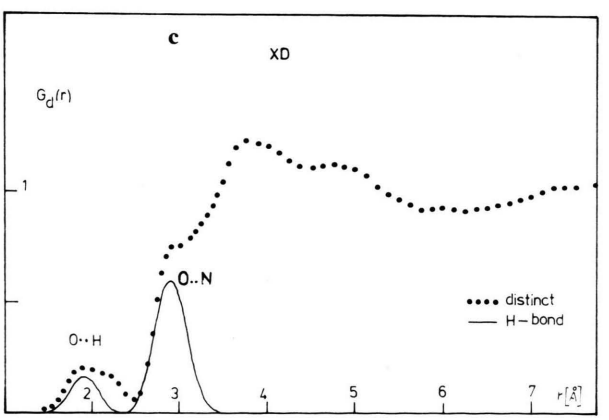

Fig. 3. The $H_d(k)$ distinct neutron, electron and X-ray structure functions of liquid formamide. The full lines represent the fitted contributions of the O...N and O...H H-bond interactions.

Fig. 4. The distinct pair correlation functions. The full lines show the contribution of H-bond interactions.

The resulting set of parameters for O...N and O...H bond interactions calculated from neutron, electron and X-ray structure functions show an overall good agreement. The mean O...N and O...H bond distances are 2.9 Å and 1.9 Å and the average number of H-bonds per monomer is four. These values of mean distances allow to estimate an average N–H...O bond angle of about 10 degrees.

The remaining differences between the $H_d(k)$ and $H_{\text{H-bond}}$ distinct structure functions seen in Fig. 3, are ascribable either to spatial correlations between C, O, and N sites of the formamide molecules or to orientational correlations between molecules. The further analysis of the distinct structure functions of the liquid formamide including the dimer formation will be published in a forthcoming paper.

Acknowledgements

Thanks are due to Mr. P. Kovács for computational assistance, Dr. T. Radnai for discussions, Mrs. A. Eke and Mr. L. Haklik for technical help and Mrs. É. Tarlós and Mrs. M. Lukácsy for preparation of the manuscript. We are grateful to the Deutsche Forschungsgemsinschaft and the Hungarian Academy of Sciences for financing this joint project. Support by the Fonds der Chemischen Industrie is gratefully acknowledged.

[1] M. Kitano and K. Kuchitsu, Bull. Chem. Soc. Japan **47,** 67 (1974).
[2] J. Ladell and B. Post, Acta Cryst. **7,** 559 (1954).
[3] J. F. Hinton and K. H. Ladner, J. Magn. Reson **6,** 586 (1972).
[4] H. Siegbahn, L. Asplund, P. Kelfve, K. Harmin, L. Karlsson, and K. Siegbahn, J. Electrosc. Relat. Phenom. **5,** 1059 (1974).
[5] A. Pullman, H. Berthod, C. Giessner-Prettre, J. F. Hinton, and D. Harpool, J. Amer. Chem. Soc. **97,** 6956 (1975).
[6] D. J. Gardiner, A. J. Lees, and B. P. Straughan, J. Mol. Struct. **53,** 15 (1979).
[7] R. J. De Sando and G. H. Brown, J. Phys. Chem. **72,** 1088 (1968).
[8] H. Ohtaki, A. Funaki, G. J. Reibnegger, and B. M. Rode, Conf. Abstr. IS_4I, Minoo, Osaka 1982.
[9] E. Kálmán, S. Lengyel, L. Haklik, and A. Eke, J. Appl. Cryst. **7,** 442 (1974).
[10] E. Kálmán, P. Kovács, L. Haklik, and G. Pálinkás, J. Phys. E; Sci. Instrum. **11,** 361 (1978).
[11] E. Kálmán, G. Pálinkás, and P. Kovács, Mol. Phys. **34,** 505 (1977).
[12] H. Bertagnolli, P. Chieux, and M. D. Zeidler, Mol. Phys. **32,** 759 (1976).
[13] H. Bertagnolli and M. D. Zeidler, Mol. Phys. **35,** 177 (1978).
[14] H. Bertagnolli, P. Chieux, F. J. Wissmann, and M. D. Zeidler, to be published.
[15] F. Hajdu, S. Lengyel, and G. Pálinkás, J. Appl. Cryst. **5,** 395 (1972).
[16] B. T. M. Willis, Chemical Applications of Thermal Neutron Scattering, University Press, Oxford 1973.
[17] International Tables for Crystallography, Vol. **4,** Kynoch Press, Birmingham 1974.
[18] A. H. Narten and S. I. Sandler, J. Chem. Phys. **71,** 2069 (1979).
[19] A. H. Narten, J. Chem. Phys. **65,** 573 (1976).
[20] S. I. Sandler and A. H. Narten, Mol. Phys. **32,** 1543 (1976).